Crystal and Molecular Structure† of Bis(tetraphenylphosphonium) Bis(1,2-dicyanoethylene-1,2-dithiolato)oxovanadate(IV). Its Single-crystal Electron Spin Resonance as a Pure Compound and Diluted in the Isomorphous Molybdenum(IV) Compound

David Collison, Frank E. Mabbs,* and John Temperley
Department of Chemistry, University of Manchester, Manchester M13 9PL
George Christou and John C. Huffman
Department of Chemistry and the Molecular Structure Center, Indiana University, Bloomington, Indiana 47405, U.S.A.

The crystal structure of $[PPh_4]_2[VO(mnt)_2]$ (mnt = 1,2-dicyanoethylene-1,2-dithiolate) has been determined at −154 °C by *X*-ray crystallographic methods. The compound crystallises in the monoclinic space group $P2_1/n$ with a = 11.176(3), b = 15.254(5), c = 14.319(4) Å, β = 97.62(1)°, and Z = 2. The anion is disordered about the inversion centre with 50% occupancy of each site. The anion has approximately square-pyramidal geometry with dimensions: V–O 1.579(10), V–S(3') 2.356(4), V–S(3) 2.372(3), V–S(4) 2.360(3), and V–S(4') 2.407(3) Å. Single-crystal e.s.r. spectra at room temperature and *Q*-band frequencies gave the spin-Hamiltonian parameters: g_1 = 1.970 ± 0.002, g_2 = 1.987 ± 0.002, g_3 = 1.988 ± 0.002, A_1 = (−42.5 ± 1.0) × 10^{-4}, A_2 = (−45.5 ± 1.0) × 10^{-4}, and A_3 = (−136.6 ± 1.0) × 10^{-4} cm^{-1}; g_1 and A_3 are coincident but g_2 and g_3 rotate by 6° from A_1 and A_2 respectively. Similarly for $[PPh_4]_2[(Mo, V)O(mnt)_2]$: g_1 = 1.971 ± 0.001, g_2 = 1.986 ± 0.001, g_3 = 1.989 ± 0.001, A_1 = (−40.3 ± 0.3) × 10^{-4}, A_2 = (−47.4 ± 0.3) × 10^{-4}, A_3 = (−136.3 ± 0.3) × 10^{-4} cm^{-1}, and $Q' = 3e^2qQ/4I(2I-1) = -(0.09 \pm 0.05) \times 10^{-4}$ cm^{-1}; g_1 and A_3 are coincident and g_2 and g_3 rotated 5.5° from A_1 and A_2 respectively. The g and A tensors have been analysed *via* both angular overlap and by constrained minimisation of a composite function of the expressions for the spin-Hamiltonian parameters to estimate the *d*-orbital mixing in the complex.

We are currently interested in the chemical, structural, and electronic properties of oxovanadium(IV) complexes, particularly those ligated by sulphur donor atoms.[1,2] Although many areas of oxovanadium(IV) chemistry are well explored there are relatively few structurally characterised compounds with sulphur donor ligands. Similarly, the detailed e.s.r. properties of such systems have not been widely studied.[2] Although $[VO(mnt)_2]^{2-}$, where mnt = 1,2-dicyanoethylene-1,2-dithiolate(maleonitriledithiolate), has been known for some time[3] it has not been structurally characterised. Similarly, apart from the report[4] of the single-crystal e.s.r. spectrum of $[PPh_3Me]_2[VO(mnt)_2]$ diluted in the chemically dissimilar host $[PPh_3Me]_2[TiO(C_2O_4)_2]$, e.s.r. studies have only been reported for fluid and frozen solutions.[4] The spin-Hamiltonian parameters on the above diluted system do not agree particularly well with those reported from solutions in 1:1 CH_2Cl_2–*NN*-dimethylformamide (dmf).[4]

In view of this difference and the known instability of $[VO(mnt)_2]^{2-}$ already reported,[4] and confirmed by our work, we now report the *X*-ray structural characterisation of $[PPh_4]_2[VO(mnt)_2]$ (**1**) and the single-crystal e.s.r. spectrum of (**1**) as a pure material and diluted in the isomorphous $[PPh_4]_2[MoO(mnt)_2]$.

Experimental

Preparations.—$[PPh_4]_2[VO(mnt)_2]$ (**1**) was prepared according to the method of McCleverty *et al.*[3] It was crystallised by layering dried dmf onto a dried saturated solution of (**1**) in methanol under dinitrogen. After several days brown rectangular plates formed. $[PPh_4]_2[MoO(mnt)_2]$ was prepared by the method of Boyde[5] and the product recrystallised from dry methanol–dmf. Single crystals of $[PPh_4]_2[MoO(mnt)_2]$ containing *ca.* 3% vanadium, (**2**), were grown by co-crystallisation with (**1**) as described above for the pure compound.

Methanol was dried by refluxing with magnesium metal and a little iodine, and dmf by storage over Linde-type 4A molecular sieves.

X-Ray Crystallography and Structure Solution of (**1**).—Data were collected at *ca.* −154 °C; details of the diffractometry, low-temperature facilities, and computational procedures employed by the Molecular Structure Center at Indiana University are available elsewhere.[6]

A systematic search of a limited hemisphere of reciprocal space located a set of diffraction maxima with monoclinic symmetry and with systematic absences corresponding to the unique space group $P2_1/n$. Subsequent solution and refinement of the structure confirmed this choice. Data were collected using a continuous θ—2θ scan technique and the data were reduced in the usual manner. Data collection parameters are summarised in Table 1.

The structure was solved[6] by a combination of direct methods (MULTAN 78) and Fourier techniques, and refined by full-matrix least squares. Non-hydrogen atoms were readily located and were refined with anisotropic thermal parameters. Molecular packing within the crystal is dominated by the large tetraphenylphosphonium ion and the mnt ligands.

This results in the anion lying on a crystallographic inversion centre. As a direct consequence the VO group is disordered about the inversion centre with exactly 50% occupancy of each site. Many of the hydrogen atom positions were visible in a difference Fourier map phased on the non-hydrogen

† *Supplementary data available:* see Instructions for Authors, *J. Chem. Soc., Dalton Trans.*, 1988, Issue 1, pp. xvii—xx.

Table 1. Crystallographic data for $[PPh_4]_2[VO(mnt)_2]$

Empirical formula	$C_{56}H_{40}N_4OP_2S_4V$
Crystal system	Monoclinic
Crystal dimensions/mm	0.16 × 0.24 × 0.30
Space group	$P2_1/n$
Cell dimensions (at −154 °C; 30 reflections)	
a/Å	11.176(3)
b/Å	15.254(5)
c/Å	14.319(4)
β/°	97.62(1)
Z	2
U/Å^3	2 420(2)
D_c/g cm^{-3}	1.408
λ(Mo-K_α)/Å	0.710 69
F(000)	1 058
Relative molecular mass/g mol^{-1}	1 026.09
Linear absorption coefficient/cm^{-1}	4.729
Scan speed/° min^{-1}	4.0
Scan width/°	2.0 + dispersion
Scan range/°	$6 \leqslant 2\theta \leqslant 40$
Unique intensities	2 251
Observed intensities	1 975 [$F > 2.33\sigma(F)$]
R^a	0.0671
R'^b	0.0768
Goodness of fit	1.46

^{a} $R = \Sigma||F_o| - |F_c||/\Sigma|F_o|$. ^{b} $R' = (\Sigma w||F_o| - |F_c||^2/\Sigma wF_o^2)^{\frac{1}{2}}$, where $w = 1/\sigma(F_o)$.

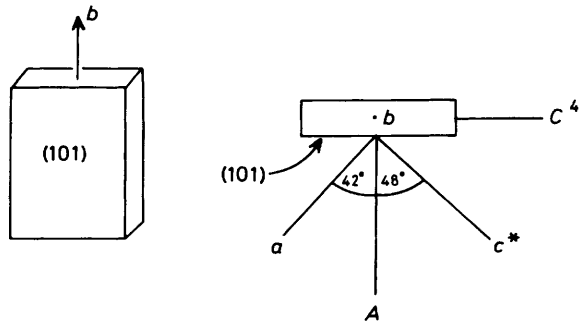

Figure 1. Crystal morphology and relationship between crystal axes and axes used for e.s.r. measurements

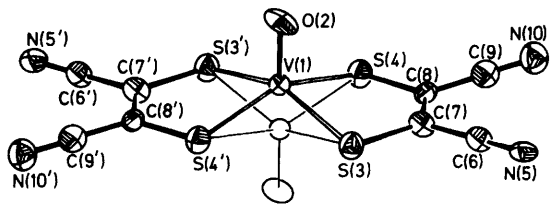

Figure 2. Structure of the $[VO(mnt)_2]^{2-}$ ion and atomic numbering

parameters. The positions of all hydrogens were calculated and placed in fixed idealised positions (C–H = 0.95 Å) for the final refinement cycles. The hydrogen atoms were assigned a thermal parameter of 0.1 + B_{iso} of the carbon atom to which they were bound. A final difference Fourier map was essentially featureless with the largest peak being 0.50 e Å^{-3}. No absorption correction was deemed necessary or performed. Final values of the discrepancy indices R and R' are in Table 1.

Spectra.—First-derivative e.s.r. spectra were obtained at room temperature on oriented single crystals of (**1**) and (**2**) at *Q*-band frequencies. The single crystals were oriented so that spectra could be obtained in the crystal planes *Ab*, *bC*, and *AC* (see Figure 1 for the crystal morphology and the relationship between the measurement and crystallographic axes). The e.s.r. spectrometer was a Varian E112 and the methods for obtaining the single-crystal spectra have been reported previously.[7]

Electronic absorption spectra were obtained at room temperature between 1500 and 300 nm on solutions in CH_2Cl_2, dmf, or on poly(dimethylsiloxane) mulls using a Varian 2390 spectrophotometer.

Resonance-Raman spectra were obtained at room temperature using a Spex 1403 085m double-beam spectrometer with a KBr disc sample.

Table 2. Fractional atomic co-ordinates (× 10^4) for the non-hydrogen atoms of $[PPh_4]_2[VO(mnt)_2]$

Atom	x	y	z
V(1)	4 687(2)	4 734(2)	−180(2)
O(2)	3 850(9)	4 003(7)	−709(7)
S(3)	6 318(2)	3 952(1)	677(2)
S(4)	3 913(2)	4 909(1)	1 270(2)
N(5)	6 923(6)	2 649(5)	2 881(5)
C(6)	6 431(7)	3 144(6)	2 384(6)
C(7)	5 788(8)	3 766(5)	1 738(6)
C(8)	4 779(7)	4 176(5)	1 992(5)
C(9)	4 455(7)	4 010(6)	2 904(7)
N(10)	4 172(7)	3 890(5)	3 648(6)
P(11)	4 989(2)	501(1)	2 054(1)
C(12)	6 391(7)	773(5)	1 639(5)
C(13)	6 383(8)	1 152(6)	752(6)
C(14)	7 430(8)	1 388(6)	433(6)
C(15)	8 543(7)	1 256(5)	983(6)
C(16)	8 550(8)	889(5)	1 860(6)
C(17)	7 491(7)	639(5)	2 194(6)
C(18)	4 904(7)	908(5)	3 227(5)
C(19)	4 791(8)	734(7)	3 968(7)
C(20)	5 674(8)	989(8)	4 861(7)
C(21)	4 659(9)	1 436(6)	5 048(6)
C(22)	3 773(8)	1 607(6)	4 309(7)
C(23)	3 904(8)	1 353(6)	3 407(6)
C(24)	4 791(7)	−663(5)	2 055(5)
C(25)	5 475(7)	−1 227(5)	1 571(6)
C(26)	5 231(8)	−2 109(6)	1 527(6)
C(27)	4 310(8)	−2 445(5)	1 974(6)
C(28)	3 636(8)	−1 913(6)	2 485(7)
C(29)	3 889(7)	−1 004(6)	2 510(6)
C(30)	3 782(7)	999(5)	1 282(5)
C(31)	1 860(7)	907(6)	308(6)
C(32)	1 901(7)	1 782(5)	106(6)
C(33)	2 786(8)	2 269(6)	481(6)
C(34)	3 816(7)	1 888(5)	1 088(6)
C(35)	2 788(8)	503(6)	905(7)

Results and Discussion

Crystal and Molecular Structure of $[PPh_4]_2[VO(mnt)_2]$ (**1**).—Final atomic co-ordinates for the non-hydrogen atoms are in Table 2. The structures of the anion and cation, along with the atomic numbering, are in Figures 2 and 3, respectively. The $[PPh_4]^+$ cation consists of a slightly distorted tetrahedral geometry about the phosphorus atom but otherwise there are no unusual features.

The bond distances and angles for the $[VO(mnt)_2]^{2-}$ ion are in Table 3. This anion has the anticipated essentially square-pyramidal geometry. The actual molecular symmetry of the anion closely approaches C_2 or C_{2v} point symmetry; however it is forced to possess crystallographic C_i symmetry which disorders the VO group about two positions with equal

Table 3. Bond distances (Å) and angles (°) for $[VO(mnt)_2]^{2-}$ *

V(1)–V(1′)	1.146(5)	S(3)–C(7)	1.720(8)
V(1)–S(3′)	2.356(4)	S(4)–C(8)	1.725(8)
V(1)–S(3)	2.372(3)	N(5)–C(6)	1.126(10)
V(1)–S(4)	2.360(3)	N(10)–C(9)	1.162(10)
V(1)–S(4′)	2.407(3)	C(6)–C(7)	1.443(13)
V(1)–O(2)	1.579(10)	C(7)–C(8)	1.377(11)
		C(8)–C(9)	1.418(12)
V(1)–V(1′)–S(3)	76.77(27)	N(5)–C(6)–C(7)	178.9(9)
V(1)–V(1′)–S(4)	73.83(25)	S(3)–C(7)–C(6)	118.1(6)
V(1)–V(1′)–O(2)	177.9(5)	S(3)–C(7)–C(8)	123.1(7)
S(3)–V(1)–S(3′)	151.96(12)	C(6)–C(7)–C(8)	118.9(7)
S(3)–V(1)–S(4)	85.86(11)	S(4)–C(8)–C(7)	123.2(6)
S(4′)–V(1)–S(4)	152.22(12)	S(4)–C(8)–C(9)	118.2(6)
S(4)–V(1)–O(2)	103.7(4)	C(7)–C(8)–C(9)	118.6(7)
V(1)–S(3)–V(1′)	28.04(12)	N(10)–C(9)–C(8)	178.6(9)
V(1)–S(3)–C(7)	101.5(3)	O(2)–V(1)–S(3)	104.9(4)
V(1)–S(4)–V(1′)	27.79(12)	O(2)–V(1)–S(3′)	103.1(4)
V(1)–S(4)–C(8)	99.9(3)	O(2)–V(1)–S(4′)	104.0(4)

* Primed atoms are related to the corresponding unprimed atom *via* the centre of symmetry.

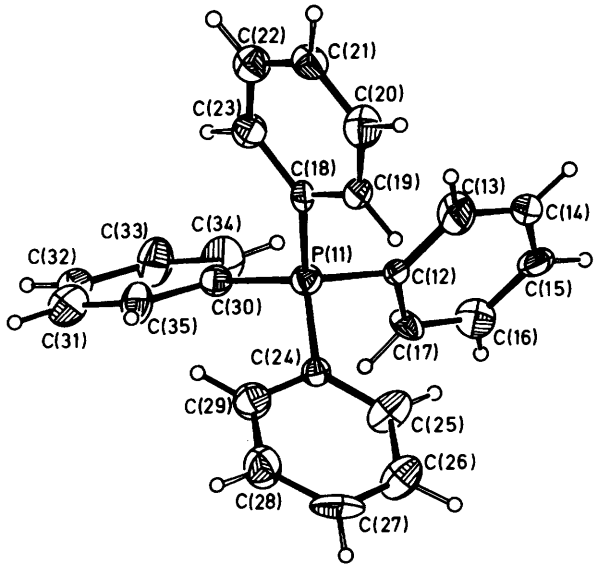

Figure 3. Structure of the $[PPh_4]^+$ ion and atomic numbering

occupancy. Since this disorder is well resolved, the e.s.d.s allow comparison with other structures. A comparison with data obtained from the Cambridge Crystallographic Files[8] shows that the vanadium–oxygen bond length falls within the range of values found for other oxovanadium(IV) compounds. However, it is shorter than that in the other structurally characterised anion containing thiolato sulphur donors,[1] $[VO(edt)_2]^{2-}$ where edt = ethane-1,2-dithiolate. This implies a greater degree of vanadium–oxygen π bonding in (**1**) compared to the edt species. However, the mean vanadium–sulphur bond length (2.376 Å) is comparable to that in $[VO(edt)_2]^{2-}$ indicating no significant effect from this putative increased vanadium–oxygen π binding on these distances. The mean O–V–S angle is also comparable to that in $[VO(edt)_2]^{2-}$, but the individual angles cover a much narrower range than in this latter anion. The bond distances and angles within the mnt ligands show no unusual features and fall within the ranges observed in other *d*-transition metal–mnt complexes.[8]

Table 4. Electronic absorption spectral data of (**1**)

Medium	Frequency of band maxima ($\times 10^{-3}$ cm^{-1})	Absorption coefficient, ε/dm^3 mol^{-1} cm^{-1}
CH_2Cl_2	10.50	160
	17.50	250
	25.64	13 600
	29.80	9 800
dmf	10.58	140
	17.40	200
	25.64	18 000
Poly(dimethylsiloxane) mull	10.30	0.9 *
	17.50	1.4 *
	23.60	1.7 *
	29.40	2.1 *

* Relative absorbance.

Electronic Absorption Spectra.—The electronic absorption spectral data of (**1**) in CH_2Cl_2, dmf, or a poly(dimethylsiloxane) mull are in Table 4. There is reasonable agreement between the band positions in each of these media and with those reported previously.[4] The first two bands are readily assignable to *d–d* transitions based on their energies in comparison to other oxovanadium(IV) compounds[9] and on their absorption coefficients. In addition a room-temperature resonance-Raman spectrum with exciting radiation of 17 368 cm^{-1} exhibits a two-membered vibrational progression with frequencies 312 and 624 cm^{-1}. A vibrational frequency of 312 cm^{-1} is consistent with a vanadium–sulphur stretching frequency, strongly suggesting that the band at 17 500 cm^{-1} is assignable to the transition between the mainly $d^*_{x^2-y^2}$ and the mainly d^*_{xy} orbitals (see later). The assignment of the other two bands is less certain. Based on previous observations[9] from low-temperature polarised single-crystal and mull spectra that five-co-ordinate oxovanadium(IV) complexes had all the *d–d* bands below 26 000 cm^{-1}, on the relative absorbances in the mull spectra, and on the assignment[2] of the $d^*_{x^2-y^2} \rightarrow d^*_{z^2}$ transition at 25 000 cm^{-1} in $[VO(edt)_2]^{2-}$, we propose that the band at 23 600 cm^{-1} in the mull spectrum contains the transition between the mainly $d^*_{x^2-y^2}$ to the mainly $d^*_{z^2}$ orbitals. However, the apparent shift and the large absorption coefficient of the third band in solution suggests a charge-transfer component for this band also. Similarly the large absorption coefficient of the band at *ca.* 29 500 cm^{-1} suggests that it is charge transfer in origin.

E.S.R. Spectra.—In crystals of both (**1**) and (**2**) eight-line patterns were observed for two magnetically inequivalent molecules in the crystal *Ab* plane but only one type in both the *bC* and *AC* planes. The differences in the spectra between (**1**) and (**2**) at equivalent orientations was the much narrower peak–peak linewidths and the observation of forbidden vanadium $\Delta m_I = 1$ transitions in (**2**). At some orientations small corrections to the g^2 tensor elements were necessary due to second-order ^{51}V hyperfine effects. These corrections were made by successive approximations in a similar manner to that described by Atherton and Winscom;[4] the effectiveness of the corrections was verified by simulation of the single-crystal spectra. The corrected g^2 and K^2g^2 tensor elements were treated according to the methods of Schonland[10] and Lund and Vanngard[11] to give the principal values and their direction cosines with respect to the crystal *A*, *b*, and *C* axes, see Table 5. The simulation of the powder and single-crystal spectra of (**2**) was based on methods outlined previously.[12] The simulation of the powder spectrum gave good agreement for alternative I, see Figure 4, and henceforth we assume this alternative to apply to

Table 5. Principal g and A tensor elements and their direction cosines with respect to the crystal axes A, b, and C

(1) $[PPh_4]_2[VO(mnt)_2]$		Alternative I				Alternative II		
		A	b	C		A	b	C
g_1	1.970 ± 0.002	0.6853	−0.7282	−0.0121	1.970 ± 0.002	0.6848	−0.7277	−0.0391
g_2	1.987 ± 0.002	−0.6131	−0.5858	0.5301	1.987 ± 0.002	0.6848	0.6610	−0.3070
g_3	1.988 ± 0.002	0.3931	0.3558	0.8479	1.988 ± 0.002	−0.2492	−0.1834	−0.9509
$10^4A/cm^{-1}$								
A_1	−42.5 ± 1.0	−0.5746	−0.5386	0.6163	−42.5 ± 1.0	−0.5903	−0.5522	0.5887
A_2	−45.5 ± 1.0	0.4421	0.4273	0.7875	−45.5 ± 1.0	0.4230	0.4095	0.8083
A_3	−136.6 ± 1.0	0.6874	−0.7262	0.0062	−136.6 ± 1.0	0.6874	−0.7262	0.0082
(2) $[PPh_4]_2[(Mo, V)O(mnt)_2]$								
g_1	1.971 ± 0.001	0.6892	−0.7231	−0.0461	1.971 ± 0.001	−0.6885	0.7222	0.0669
g_2	1.986 ± 0.001	−0.5533	−0.5663	0.6108	1.987 ± 0.001	−0.5715	−0.5970	0.5630
g_3	1.989 ± 0.001	0.4678	0.3954	0.7904	1.988 ± 0.001	−0.4465	−0.3494	−0.8238
$10^4A/cm^{-1}$								
A_1	−40.3 ± 0.3	−0.5230	−0.5094	0.6834	−41.5 ± 0.3	−0.5262	−0.5174	−0.6749
A_2	−47.4 ± 0.3	−0.5027	−0.4632	−0.7299	−46.3 ± 0.3	−0.4995	−0.4543	0.7377
A_3	−136.3 ± 0.3	0.6883	−0.7253	−0.0138	−136.6 ± 0.3	0.6883	−0.7252	0.0194

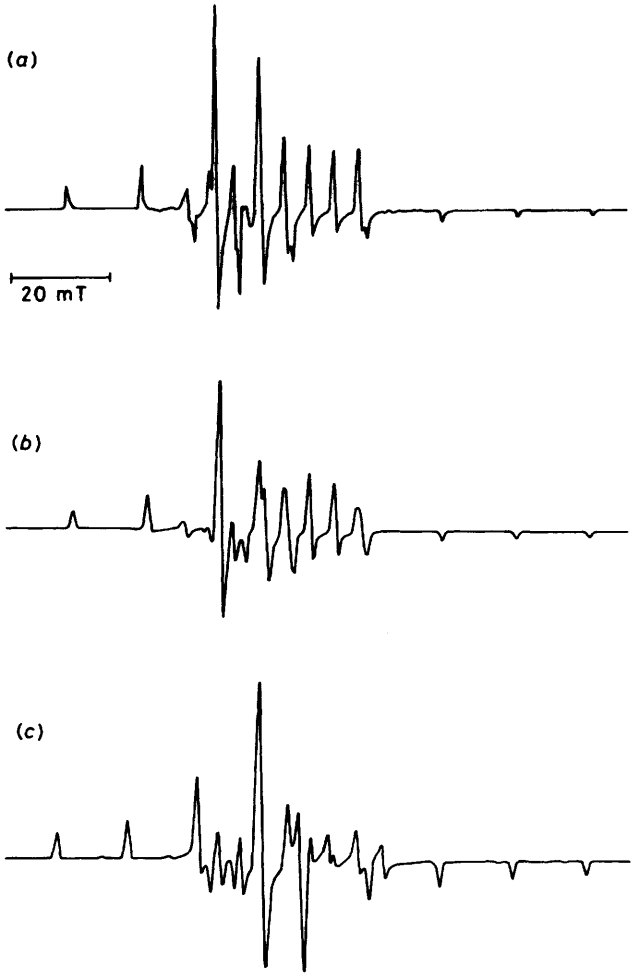

Figure 4. Comparison of (*a*) the room-temperature powder spectrum of (**2**), the simulated spectrum (*b*) alternative I and (*c*) alternative II in Table 5. In both (*b*) and (*c*) linewidth parameters are $w_1 = w_2 = w_3 = 0.8$ mT. Microwave frequency $\nu = 35.074$ GHz; each spectrum starts at 1.2 T

Table 6. Angles (°) between the axes of the g and A tensors

	$[PPh_4]_2[VO(mnt)_2]$			$[PPh_4]_2[(Mo, V)O(mnt)_2]$		
	A_1	A_2	A_3	A_1	A_2	A_3
g_1	90.5	91.0	1.1	91.4	88.7	1.9
g_2	6.0	96.0	89.6	5.6	84.6	88.8
g_3	84.0	6.5	89.0	84.6	174.4	88.6

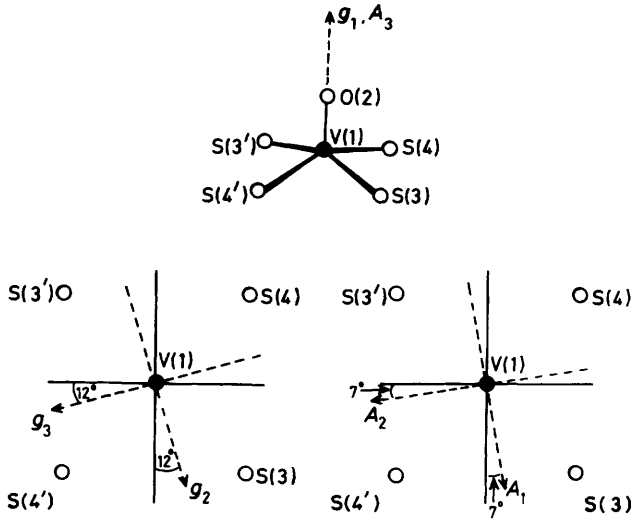

Figure 5. Orientation of the principal g and A tensors with respect to the structure of $[VO(mnt)_2]^{2-}$ for alternative I. The solid lines are the bisectors of the S–V–S angles for the sulphur atoms projected into the plane perpendicular to the VO vector

both (**1**) and (**2**). The principal g and A tensors are in good agreement between (**1**) and (**2**) indicating no significant changes on dilution. They also agree well with those reported[4] for a frozen CH_2Cl_2–dmf solution of $[PPh_3Me]_2[VO(mnt)_2]$. However, the principal g and A values differ significantly from those obtained using $[PPh_3Me]_2[TiO(C_2O_4)_2]$ as a diluent,[4] suggesting a change in the nature of the diluted species in this latter study. The angles between the principal g and A tensor

elements are in Table 6 and their relationship to the molecular geometry is shown in Figure 5. Although there is approximately 2° between g_1 and A_3, each of these individual elements is parallel to the V–O vector to within experimental error. We will assume such coincidence for subsequent interpretation. The principal g and A tensor elements perpendicular to V–O are rotated relative to each other by *ca.* 5.5°. These two features indicate that the $[VO(mnt)_2]^{2-}$ ion approximates most nearly to C_2 point symmetry.[13,14]

Relationship between the Electronic Structure, E.S.R. Parameters, and the Electronic Absorption Spectrum of $[PPh_4]_2[VO(mnt)_2]$.—Assuming the anion to belong to the point group C_2, with the two-fold axis parallel to V=O, the allowed d-orbital mixings are as shown below, where α,β,γ,δ, and ε are the metal

$$\psi_1 = \alpha(a_1 d_{x^2-y^2} + b_1 d_{xy} + c_1 d_{z^2})$$
$$\psi_2 = \alpha(a_2 d_{x^2-y^2} + b_2 d_{xy} + c_2 d_{z^2})$$
$$\psi_3 = \gamma(e_3 d_{xz} + f_3 d_{yz})$$
$$\psi_4 = \delta(e_4 d_{xz} + f_4 d_{yz})$$
$$\psi_5 = \varepsilon(a_5 d_{x^2-y^2} + b_5 d_{xy} + c_5 d_{z^2})$$

coefficients in the antibonding molecular orbitals.

Table 7. An example of the parameters required by the angular overlap model to reproduce the e.s.r. data

Ligand atom	θ/°	φ/°	$10^{-4}e_\sigma$/cm^{-1}	$10^{-4}e_\pi$/cm^{-1}
O(2)	0.0	0.0	2.150	0.980
S(3)	104.0	306.5	0.790	0.095
S(3′)	104.0	126.5	0.790	0.095
S(4)	104.3	33.0	0.790	0.095
S(4′)	104.3	213.0	0.790	0.095

Orbital	Calculated relative energy/cm^{-1}	*d*-Orbital mixing coefficients a_i	b_i	c_i	d_i	e_i
ψ_1	0	0.9363	−0.3500	0.0280	—	—
ψ_2	17 480	−0.3503	−0.9366	0.0057	—	—
ψ_3	10 677	—	—	—	−0.9924	0.1231
ψ_4	10 183	—	—	—	−0.1231	−0.9924
ψ_5	23 861	−0.0242	−0.0151	0.9996	—	—

These d-orbital mixings plus the parameters $\alpha = 0.98 \pm 0.01$, $\beta = 0.73 \pm 0.01$, $\gamma = 0.83 \pm 0.02$, $\delta = 0.75 \pm 0.02$, $\varepsilon = 0.71 \pm 0.03$, $P = 109.0 \pm 0.4 \times 10^{-4}$ cm^{-1}, and $\xi_v = 135.5 \pm 0.8$ cm^{-1} give calculated spin-Hamiltonian parameters $g_{zz} = 1.971 \pm 0.001$, $g_{xx} = 1.987 \pm 0.001$, $g_{yy} = 1.987 \pm 0.001$; $A_{zz} = -(136.0 \pm 0.1) \times 10^{-4}$, $A_{xx} = -(46.6 \pm 0.1) \times 10^{-4}$, $A_{yy} = -(41.5 \pm 0.1) \times 10^{-4}$, $A_{xy} = (0.7 \pm 0.1) \times 10^{-4}$, and $A_{yx} = (1.0 \pm 0.1) \times 10^{-4}$ cm^{-1}.

Within the approximation of neglecting contributions from the sulphur donor atoms we have estimated the metal mixing coefficients and molecular orbital coefficients by both an angular overlap and the constrained minimisation models described for $[VO(mquin)_2]$ (mquin = 2-methylquinolin-8-olate).[14] In these calculations we have used the previous[14] criteria for the acceptability of the fit to the electronic absorption spectrum from the angular overlap model and for the equality, inequality, and range constraints in the minimisation treatment.

The ranges of angular overlap parameters which fit the solid-state electronic spectrum to within ± 500 cm^{-1} are for the terminal oxo, e_σ = 21 000—22 000 cm^{-1}, $e_{\pi x} = e_{\pi y}$ = 9 400—10 100 cm^{-1} and for the sulphur donor atoms, e_σ = 7 700—8 100 cm^{-1}, $e_{\pi x}$, $e_{\pi y}$ = 900—1 000 cm^{-1}. An example of a set of parameters which gives an acceptable calculation of the e.s.r. parameters is in Table 7. The results of the constrained minimisation treatment are in Table 8. The two methods give good agreement between the d-orbital mixing coefficients, metal molecular orbital coefficients, P, and ξ_V.[2]

The angular overlap parameter for the terminal oxo group is consistent with it being both a good σ and π donor. By comparison with $[VO(mquin)_2]$ the terminal oxo group in $[VO(mnt)_2]^{2-}$ is acting as a better σ donor but a weaker π donor. The relative σ donor strengths are consistent with the V–O bond lengths {1.600(8) Å in $[VO(mquin)_2]$ and 1.579(10) Å in (**1**)} although there are large standard deviations in these lengths. The e_σ and e_π parameters for the sulphur donor atoms also indicate strong σ donor and significant π donor properties. The values of P, and the associated values of ξ_V, required to fit the e.s.r. data indicate a formal charge on the vanadium close to +1.[15,16] This formal charge is similar to that deduced[2] from e.s.r. measurements on the sulphur ligated $[VE(edt)_2]^{2-}$, where E = O or S, but lower than that reported (between +2.0 and +1.5) for $[VO(mquin)_2]$[14] which contains oxygen and nitrogen donor ligands. The smaller values of the metal molecular orbital coefficients β,γ, and δ in (**1**) compared with $[VO(mquin)_2]$ are also consistent with the lower charge on the metal in the former being due to increased covalency.

In crystals of (**2**) the effect of the ^{51}V nuclear Zeeman and quadrupole interactions allows the observation of the formally forbidden $\Delta m_I = \pm 1$ transitions which occur as doublets at magnetic fields between those for the allowed transitions; for an example see Figure 6. These single-crystal spectra were analysed by spectrum simulation[12] *via* the spin-Hamiltonian (*1*), where $Q' = 3e^2qQ/4I(2I - 1)$.

$$\mathcal{H} = \beta_e B \cdot g \cdot \hat{S} + \hat{I} \cdot A \cdot \hat{S} + Q'[\hat{I}_z^2 - I(I+1)] - g_N\beta_N H \cdot \hat{I} \quad (1)$$

Table 8. Parameters obtained from the method of constrained minimisation

Orbital	Relative energy[a]/cm^{-1}	a_i	b_i	c_i	e_i	f_i	Molecular orbital coefficient
ψ_1		0.981	−0.190	0.035	—	—	1.00
ψ_2	17 500	0.189	0.982	−0.001	—	—	0.73
ψ_3	10 300	—	—	—	0.983	−0.184	0.86
ψ_4	10 300	—	—	—	0.184	0.983	0.72
ψ_5	23 500	−0.035	0.007	0.999	—	—	0.73

$P = 104.9 \times 10^{-4}$ cm^{-1}, $\xi_v = 128.0$ cm^{-1}

	xx	*yy*	*zz*	*xy*	*yx*
A_{ij}(obs.)[b]	−47.3	−40.4	−136.3	0.7	0.7
A_{ij}(calc.)[b]	−47.3	−40.4	−136.3	0.7	0.7
g_{ij}(obs.)	1.989	1.986	1.971	0.0	0.0
g_{ij}(calc.)	1.987	1.986	1.971	0.0	0.0

[a] Experimental values with assignments in the text which are compatible with the angular overlap calculation. [b] In units of 10^{-4} cm^{-1}.

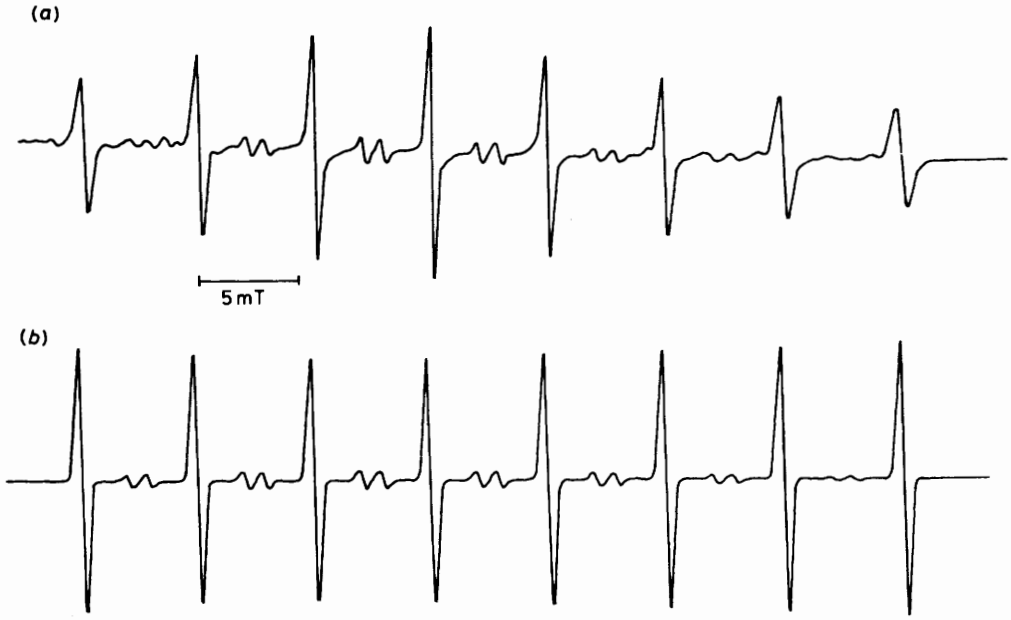

Figure 6. An example of the experimental (*a*) and simulated (*b*) spectra showing the formally forbidden $\Delta m_I = \pm 1$ transitions in the single-crystal e.s.r. spectrum of (**2**) with the magnetic field in the *AC* plane at 20° to *C*. The parameters used in the simulation are in the text

In this analysis we obtained the exact solution for the application of (1) by matrix diagonalisation. The relative intensities of all the possible transitions were computed from the resulting eigenvectors. The *g* and *A* tensors used were those in Table 5, whilst g_N was assumed to be isotropic with a value of 1.47.[17] The observed spacings and relative intensities of the forbidden doublets were satisfactorily simulated with $Q' = -(0.09 \pm 0.05) \times 10^{-4}$ cm^{-1} and quadrupole tensor axes coincident with those of the *g* tensor. The spectrum resolution did not permit a more accurate determination of Q', but the pattern of the relative intensities of the forbidden transitions throughout the spectra requires Q' to be negative. In view of the small deviation of the *g* and *A* tensors from axial symmetry it is not unreasonable to fit the spectra with an axially symmetric quadrupole tensor.

Our estimated value of Q' is a smaller negative value than that reported for the square-pyramidal compound $[VO(bzac)_2]$ diluted in $[Pd(bzac)_2]$[18] (bzac = benzoylacetylacetonate ($Q' = -0.3 \pm 0.2 \times 10^{-4}$ cm^{-1}), but is comparable with the value found in the presumed six-co-ordinate vanadium(IV) in the $Na[NH_3Me]_2[V_2W_4O_{19}]\cdot 6H_2O$ host ($Q' = -0.095 \pm 0.01 \times 10^{-4}$ cm^{-1}).[18] A smaller negative value of Q' and by implication a smaller electric-field gradient in (**2**) compared to $[VO(bzac)_2]$ may arise from the increased covalency in (**2**), particularly the π-donor properties of the mnt ligand compared to the oxygen donor, bzac.

Acknowledgements

Thanks are due to the S.E.R.C. for financial support to J. T. and F. E. M. and to the Royal Society for D. C. The work was also supported in part by NSF Grant CHE-8507748 (to G. C.), NSF Grant CHE-7709496 for the *X*-ray diffractometer, and the Bloomington Academic Computing Service.

References

1 J. K. Money, J. C. Huffman, and G. Christou, *Inorg. Chem.*, 1985, **24**, 3297.
2 J. K. Money, K. Folting, J. C. Huffman, G. Christou, D. Collison, F. E. Mabbs, and J. Temperley, *Inorg. Chem.*, 1986, **25**, 4583.
3 J. A. McCleverty, J. Locke, B. Ratcliff, and E. J. Wharton, *Inorg. Chim. Acta*, 1969, **3**, 283.
4 N. M. Atherton and C. J. Winscom, *Inorg. Chem.*, 1973, **12**, 383.
5 S. Boyde, Ph. D. Thesis, University of Manchester, 1986.
6 M. H. Chisholm, K. Folting, J. C. Huffman, and C. C. Kirkpatrick, *Inorg. Chem.*, 1984, **23**, 1021.
7 C. D. Garner, P. Lambert, F. E. Mabbs, and J. K. Porter, *J. Chem. Soc., Dalton Trans.*, 1972, 30.
8 F. H. Allen, O. Kennard, and R. Taylor, *Acc. Chem. Res.*, 1983, **16**, 146.
9 D. Collison, B. Gahan, C. D. Garner, and F. E. Mabbs, *J. Chem. Soc., Dalton Trans.*, 1980, 667 and refs. therein.
10 D. S. Schonland, *Proc. Phys. Soc., London*, 1959, **73**, 788.
11 A. Lund and T. Vanngard, *J. Chem. Phys.*, 1965, **42**, 2979.
12 D. Collison and F. E. Mabbs, *J. Chem. Soc., Dalton Trans.*, 1982, 1565; B. Gahan and F. E. Mabbs, *ibid.*, 1983, 1713.
13 D. Collison, F. E. Mabbs, J. H. Enemark, and W. E. Cleland, jun., *Polyhedron*, 1986, **5**, 423.
14 D. Collison, B. Gahan, and F. E. Mabbs, *J. Chem. Soc., Dalton Trans.*, 1987, 111.
15 B. R. McGarvey, *J. Phys. Chem.*, 1967, **71**, 51.
16 T. M. Dunn, *Trans. Faraday Soc.*, 1961, **57**, 1441; B. N. Figgis and J. Lewis, *Prog. Inorg. Chem.*, 1964, **6**, 37.
17 J. S. Griffith, 'The Theory of Transition-Metal Ions,' Cambridge University Press, 1964, p. 380.
18 R. L. Belford, D. T. Huang, and H. So, *Chem. Phys. Lett.*, 1972, **14**, 592.

Received 13*th January* 1987; *Paper* 7/063